Colloids and Interface Science Communications 4 (2015) 1–4

Contents lists available at ScienceDirect

Colloids and Interface Science Communications

journal homepage: www.elsevier.com/locate/colcom

Rapid Communication

A thermosensitive hydrogel carrier for nickel nanoparticles

Jianjia Liu [a,1], Jie Wang [a,b,c,*,1], Yiming Wang [a], Chang Liu [a], Miaomiao Jin [a], Yisheng Xu [a], Li Li [a], Xuhong Guo [a,**], Aiguo Hu [b], Tingyu Liu [c], Stephen F. Lincoln [d,**], Robert K. Prud'homme [e]

[a] State Key Laboratory of Chemical Engineering, East China University of Science and Technology, Shanghai 200237, China
[b] Shanghai Key Laboratory of Advanced Polymeric Materials, School of Materials Science and Technology, East China University of Science and Technology, Shanghai 200237, China
[c] Suzhou Industrial Park Human Resources Development Co., Ltd., Suzhou 215021, China
[d] Department of Chemistry, University of Adelaide, Adelaide, SA 5005, Australia
[e] Department of Chemical Engineering, Princeton University, Princeton, NJ 08544, USA

ARTICLE INFO

Article history:
Received 30 October 2014
Received in revised form 10 December 2014
Accepted 12 December 2014
Available online 23 December 2014

Keywords:
Heterogeneous catalysis
Hydrogels
Nanoparticles
Phase transitions

ABSTRACT

Segments of a p(NIPA-co-AMPS) hydrogel synthesized from *N*-isopropyl acrylamide (NIPA) and 2-acrylamido-2-methyl-1-propane sulfonic acid (AMPS) with *N*,*N*′-methylenebis(acrylamide) (BIS) acting as cross-linker stabilized nickel nanoparticles (Ni-NPs) of uniform size in an aqueous solution. The rate of catalysis of the borohydride reduction of 4-nitrophenol to 4-aminophenol by these nanoparticles shows a complex temperature variation consistent with the hydrogel changing from a contracted to an expanded state below a lower critical solution temperature, LCST, of ~310 K. These observations provide insights into nanoparticle stabilization and catalysis and indicate potential pathways toward stable sophisticated nanoparticle catalysts for use in aqueous solution.

Metal nanoparticles have attracted considerable interest as their chemical and physical properties differ substantially from those of bulk metals [1–5]. While these properties are of both fundamental and practical interest, their study has often been hindered by the tendency of metal nanoparticles to aggregate and precipitate from aqueous solutions which are of particular interest as water is environmentally benign. Consequently, a range of aqueous carrier systems exemplified by core–shell particles [6–10], dendrimers [11,12], hydrogels [13–17] polyelectrolyte brushes [18,19] and supramolecular structure such as cyclodextrins [20,21] has been developed. We are particularly interested in stable hydrogel carrier systems which are amenable to easy handling. Accordingly, we made the p(NIPA-co-AMPS) hydrogel from *N*-isopropyl acrylamide (NIPA) and 2-acrylamido-2-methyl-1-propane sulfonic acid (AMPS) with *N*,*N*′-methylenebis(acrylamide) (BIS) acting as cross-linker. Solid segments of this copolymer hydrogel stabilize nickel nanoparticles of uniform size in aqueous solution. The catalysis of the borohydride reduction of 4-nitrophenol to 4-aminophenol by these nanoparticles exhibits a complex temperature dependence consistent with the p(NIPA-co-AMPS) hydrogel changing from a contracted to an expanded state below a lower critical solution temperature, LCST, of ~310 K. We view these observations as precursors to a major investigation into the effects of copolymer composition and metal nanoparticle identity on a range of nanoparticle catalyzed reactions.

The synthesis of the Ni-NP-p(NIPA-co-AMPS) hydrogel was achieved by the dissolution of NIPA (1.91 g) and AMPS (1.75 g) in 12 cm^3 in water followed by the addition of BIS (0. 013 g) to act as the cross-linker and AAPH (0.01 g) to act as the initiator with thorough mixing for 10 min. The solution was injected into a glass tube which was 15 mm in diameter and 15 cm long and the open end was sealed with parafilm after which it was irradiated for 2 h with a UV–vis lamp with a 200–600 nm range with a maximum intensity at 400 nm. The tube was then carefully broken open to release the solid cylinder of p(NIPA-co-AMPS) hydrogel which was cut into 4 mm thick cylindrical sections. Unreacted reagents were removed from these sections by immersing them in gently stirred deionized water for 24 h, during which time the water was changed at 4 h intervals. The hydrogel sections were then dried to constant weight in a vacuum oven at 323.2 K. A FTIR spectrum (KBr thin section) was run on a Nicolet-iS 10 FTIR spectrometer: 1040 (m), 1385 (m), 1550 (m), 1647 (m), 3134 (s), 3422 (s) cm^{-1} (Supporting information, Fig. S1).

Circular segments of the oven-dried p(NIPA-co-AMPS) (0.044 g each) were immersed in gently stirred aqueous 0.10 mol dm^{-3} $NiCl_2$ solution at room temperature for 48 h, during which time the decreasing Ni^{2+} concentration of the solution was monitored by inductively coupled plasma atomic emission spectroscopy, ICP-AES, using an IRIS 1000 instrument, until it stabilized after ~24 h, consistent with the hydrogel absorption of Ni^{2+} being complete (the maximum weight of

* Correspondence to: J. Wang, State Key Laboratory of Chemical Engineering, East China University of Science and Technology, Shanghai 200237, China.
** Corresponding authors.
E-mail addresses: jiewang2010@ecust.edu.cn (J. Wang), guoxuhong@ecust.edu.cn (X. Guo), stephen.lincoln@adelaide.edu.au (S.F. Lincoln).
[1] These authors contributed equally to this work.

http://dx.doi.org/10.1016/j.colcom.2014.12.001

$NiCl_2$ in the hydrogel was 9.5 mg). After washing with deionized water to remove extraneous $NiCl_2$, the green hydrogel was placed in a stirred 100 cm^3 0.5 mol dm^{-3} $NaBH_4$ aqueous solution under a nitrogen atmosphere for 12 h. The now black hydrogel segments were then removed and washed with deionized water three times to remove any extraneous Ni-NP on the surface. Prior to use in the kinetic studies discussed below, these hydrogel segments were dried to constant weight in a vacuum oven at 323.2 K. To determine the Ni-NP content a segment of the Ni-NP-p(NIPA-co-AMPS) hydrogel was dried to a constant weight of 48 mg several 3.5 mg segments of which were then dissolved in separate 5 cm^3 of 11 mol dm^{-3} hydrochloric acid solutions which were analyzed for Ni^{2+} by ICP-AES. This showed the dried Ni-NP-p(NIPA-co-AMPS) to be 9% Ni-NP by mass.

Prior to commencement of each catalytic kinetic run, a 48 mg segment of vacuum oven dried Ni-NP-p(NIPA-co-AMPS) was immersed in water at the temperatures corresponding to that of the kinetic run for 24 h under nitrogen. To initiate the kinetic run the Ni-NP-p(NIPA-co-AMPS) hydrogel segment was transferred into 100 cm^3 of a thermostated and stirred aqueous solution 0.00216 and 0.216 mol dm^{-3} in 4-NP and $NaBH_4$, respectively, under nitrogen in a stoppered flask. At appropriate time intervals, 0.10 cm^3 samples of this solution were extracted and delivered into 3.0 cm^3 volumes of deionized water at room temperature and the UV–vis spectra of the solutions were recorded.

The hydrogel structure and the morphology of the Ni-NP were determined by scanning electron microscopy, SEM, using a FEI-Nova450 instrument, and by high resolution transmission electron microscopy, HRTEM, using a JEM-2100F instrument respectively. In the kinetic experiments the UV–vis spectra were recorded in thermostated 1 cm pathlength quartz cells using a SHIMADZU UV-2550 spectrophotometer.

Scanning electron microscopy (SEM) shows the vacuum oven (323.2 K) dried copolymer to have the dominant macroscopic structure shown in Fig. 1. Small segments of the p(NIPA-co-AMPS) hydrogel in stirred aqueous 0.10 mol dm^{-3} $NiCl_2$ solution at room temperature for 48 h, during which time the decreasing Ni^{2+} concentration of the bulk solution was monitored by inductively coupled plasma atomic emission spectroscopy, ICP-AES. The bulk Ni^{2+} concentration stabilized after 24 h. This is consistent with the absorption of Ni^{2+} by the p(NIPA-co-AMPS) segments being complete and the copolymer absorbing water to form a hydrogel in which the sulfonic acid groups are dissociated. Subsequent stirring of these segments in 100 cm^3 of aqueous 0.50 mol dm^{-3} $NaBH_4$ solution under nitrogen for 12 h causes them to become black as Ni^{2+} is reduced to form nickel nanoparticles, Ni-NP, in a Ni-NP-p(NIPA-co-AMPS) hydrogel.

High resolution transmission electron microscopy (HRTEM) shows a uniform distribution of Ni-NP in the Ni-NP- p(NIPA-co-AMPS) hydrogel with a narrow distribution of Ni-NP diameters centered at 26.24 nm (Fig. 2). This is consistent with a regular pore size distribution within the hydrogel and probable interactions of either the amide or sulfonate

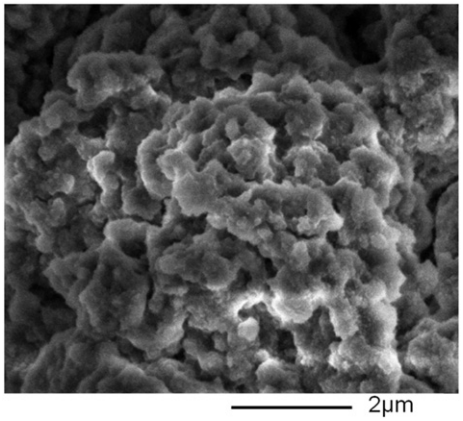

Fig. 1. SEM image of the vacuum oven dried p(NIPA-co-AMPS) copolymer.

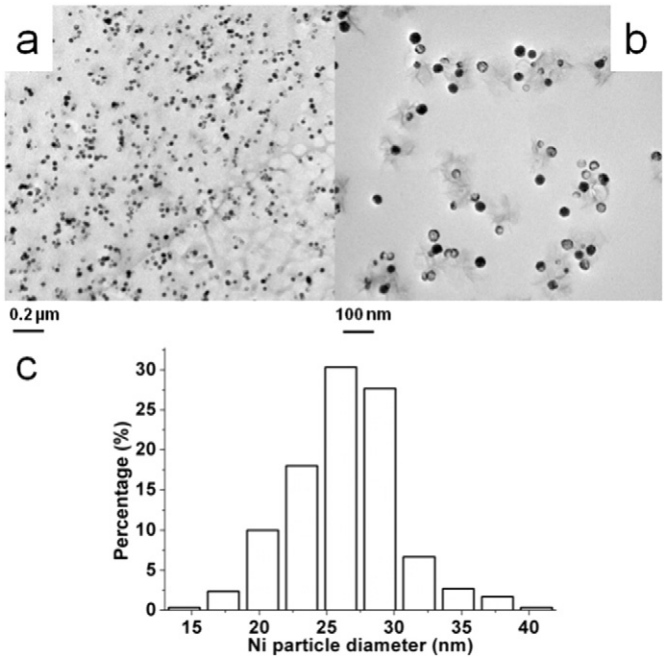

Fig. 2. HRTEM, images of Ni-NP-p(NIPA-co-AMPS) hydrogel at different magnifications in a) and b). Distribution of Ni-NP diameters are shown in c).

groups, or both, controlling Ni-NP size and preventing aggregation. The Ni-NP content of the Ni-NP-p(NIPA-co-AMPS) hydrogel segments dried to constant weight was determined to be 9% Ni-NP by mass.

In the temperature range 293.8–317.1 K the Ni-NP-p(NIPA-co-AMPS) hydrogel showed a complex temperature dependence of the swelling ratio, *SR*, defined by Eq. (1):

$$SR = (W_T - W_d)/W_d \quad (1)$$

were, W_T is the weight reached after suspension in water at temperature T and W_d is the dry weight determined over a range of temperatures by placing a weighed portion of the oven-dried hydrogel in thermostated deionized water from which it was removed and weighed at intervals until a constant weight was reached. The Ni-NP-p(NIPA-co-AMPS) hydrogel *SR* undergoes a gradual decrease as temperature increases from 293.8 K followed by a sudden decrease over the temperature range 308.9–312.0 K centered at ~310 K, the lower critical solution temperature, LCST. A constant *SR* is reached as temperature increases from 313.9 to 317.1 K (Fig. 3). Thus, the Ni-NP-p(NIPA-co-AMPS) hydrogel changes from an expanded state in the lower temperature range where it absorbs most water to a contracted state in the higher temperature range where it absorbs less water.

The borohydride reduction of 4-nitrophenol, 4-NP, to 4-aminophenol is catalyzed by metal nanoparticles [4–8] and was used here to test the catalytic capacity of the Ni-NP in the Ni-NP-p(NIPA-co-AMPS) hydrogel. In these studies the $NaBH_4$ concentration was in one hundred-fold excess over that of 4-NP such that the reduction occurred under pseudo-first order conditions. At each reaction temperature, a 48 mg segment of the Ni-NP-p(NIPA-co-AMPS) hydrogel (dried to constant weight in a vacuum oven at 323.2 K) was placed in 100 cm^3 of a thermostated and stirred aqueous solution 0.00216 and 0.216 mol dm^{-3} in 4-NP and $NaBH_4$, respectively, under nitrogen in a stoppered flask. At appropriate time intervals, 0.10 cm^3 samples of this solution were extracted and delivered into 3 cm^3 volumes of deionized water at room temperature and the UV–vis spectra of the resulting solutions were recorded (Fig. 4). The absorbance maximum at 400 nm arising from 4-nitrophenolate, 4-NP^-, decreased with time coincident with the increase in the maxima at 233 and 300 nm arising from the reduction product, 4-AP. Isosbestic points at 222, 247, 281, and 313 nm indicate that 4-NP^- and 4-AP were the

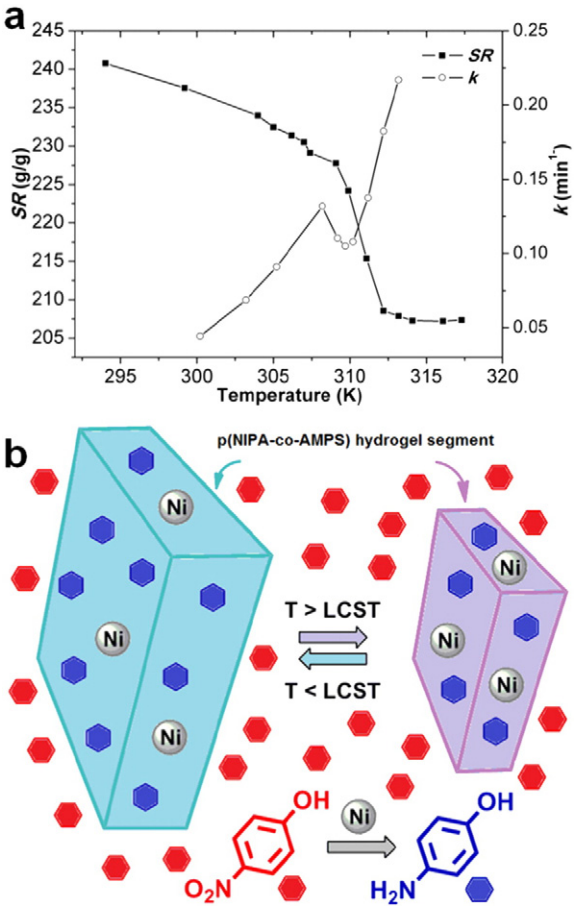

Fig. 3. (a) Swelling ratio, *SR*, of Ni-NP-p(NIPA-co-AMPS) hydrogel at different temperatures shown as closed squares. The pseudo first order rate constants, *k*, for the reduction of 4-NP at each temperature are shown as open circles. (b) Schematic diagram of thermosensitive Ni-NP-p(NIPA-co-AMPS) hydrogel in the reduction of 4-NP.

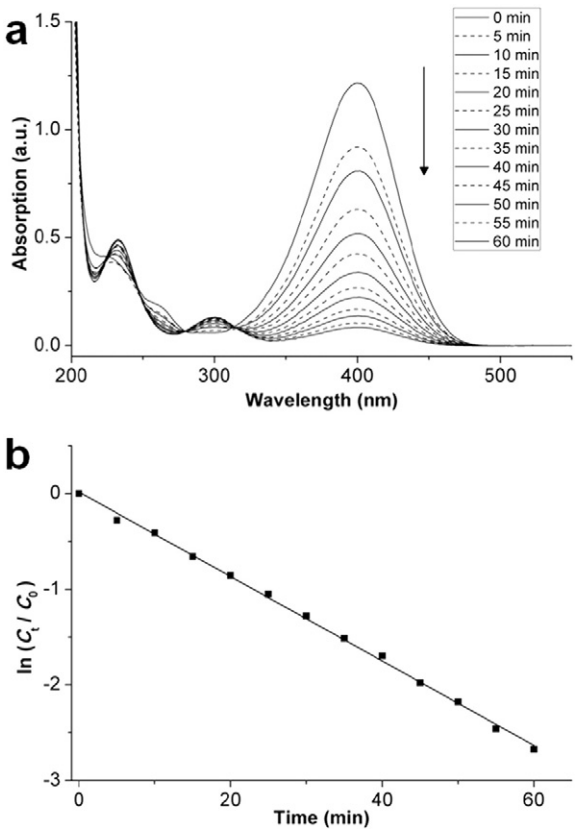

Fig. 4. (a) Time dependent UV–vis spectra for the reduction of 4-NP in the presence of a 0.048 g Ni-NP-p(NIPA-co-AMPS) hydrogel segment at 300.2 K and initial [4-NP] = 0.00216 mol dm^{-3}, [$NaBH_4$] = 0.216 mol dm^{-3}. The 4-NP absorption maxima occurs at 400 nm and those for 4-AP at 233 and 300 nm, with isosbestic points at 222, 247, 281, and 313 nm. Each sample taken was diluted as described in the text prior to its spectrum being recorded. (b) Plot of $\ln(c_t/c_0)$ versus time derived at 400 nm from the spectra in (a) where c_t and c_0 are the concentrations at time *t* and zero respectively. The derived pseudo first order rate constant, $k = 0.044 \pm 0.002$ min^{-1} (300.2 K).

dominant absorbing species in solution. The pseudo-first order reduction rate constant, *k*, was calculated through Eq. (2):

$$\ln(c_t/c_0) = -kt \tag{2}$$

where c_t and c_0 are the 4-NP concentration at time *t* and zero, respectively, determined from the 4-NP^- UV–vis absorbance (Figs. 4 and S2). (Induction periods have been observed for metal nanoparticle catalyzed 4-NP reduction [18,19,22], but were not observed in this study probably because they were shorter than the time interval between the commencement of the reaction and the first sample being taken.)

The complex temperature dependence of *k* (Fig. 3) is consistent with the combination of an Eyring temperature dependence with that of the swelling ratio, *SR*. Initially, *k* increases with temperature from 300.2 K, but within the range 308.2–311.2 K a decrease in *k* occurs coincident with the substantial decrease in the hydrogel swelling ratio, *SR*, occurring in the same temperature range (Fig. 3). This is consistent with the expanded and contracted states of the Ni-NP-p(NIPA-co-AMPS) hydrogel existing at the low and high ends of the 300.2–313.2 K temperature range, respectively, accommodating more and less 4-NP, $NaBH_4$ and water. It is also likely that the reactant diffusion rates in the contracted hydrogel are less than those anticipated at the same temperature in the expanded hydrogel. Both effects are expected to decrease the 4-NP reduction rate constant, *k*, in the contracted copolymer hydrogel by comparison with that in the expanded form. A similar shrinkage in volume and a corresponding decrease in the rate of the catalyzed reduction of 4-NP by borohydride with an increase in temperature was first observed for core–shell particles (of hydrodynamic radii ranging from 143 to 80 nm at 283.3 and 318.2 K, respectively) consisting of a polystyrene core and surrounded by a shell of poly(*N*-isopropylacrylamide) cross-linked with *N*,*N*′-methylenebis(acrylamide) containing silver nanoparticles in aqueous solution [6–8].

In conclusion, our observations indicate that a substantial degree of control may be gained over the behavior of hydrogels and their role in facilitating metal nanoparticle catalysis which may lead to sophisticated new catalysts for use in water. Future studies will involve the effect of polymer composition on the stability and size of metal nanoparticles incorporated into hydrogels, the effect of metal identity on catalysis and the study of a range of catalyzed reactions to establish a broader understanding of metal nanoparticle carrying hydrogels in catalysis.

This work was supported by the NSFC Grants 51403062, 51273063 and 20774030, the Fundamental Research Funds for the Central Universities, the higher school specialized research fund for the doctoral program (20110074110003), the China Postdoctoral Science Foundation (2013M541485), the China Scholarship Council, the Australian Research Council Grant DP110103177 and 111 Project Grant (B08021).

Appendix A. Supplementary data

Supplementary data to this article can be found online at http://dx.doi.org/10.1016/j.colcom.2014.12.001.

References

[1] C. Burda, X. Chen, R. Narayanan, M.A. El-Sayed, Chemistry and properties of nanocrystals of different shapes, Chem. Rev. 105 (2005) 1025–1102.

[2] D. Astuc, Nanoparticles and Catalysis, Wiley-VCH, Weinheim, 2007.
[3] R. Ferrando, J. Jellinek, R.L. Johnston, Nanoalloys: from theory to applications of alloy clusters and nanoparticles, Chem. Rev. 108 (2008) 845–910.
[4] Y. Lu, M. Ballauff, Thermosensitive core–shell microgels: from colloidal model systems to nanoreactors, Prog. Polym. Sci. 36 (2011) 767–792.
[5] P. Hervés, M. Pérez-Lorenzo, L.M. Liz-Marzán, J. Dzubiella, Y. Lu, M. Ballauff, Catalysis by metallic nanoparticles in aqueous solution: model reactions, Chem. Soc. Rev. 41 (2012) 5577–5587.
[6] Y. Lu, Y. Mei, M. Drechsler, M. Ballauff, Thermosensitive core–shell particles as carriers for Ag nanoparticles: modulating the catalytic activity by a phase transition in networks, Angew. Chem. Int. Ed. 45 (2006) 813–816.
[7] Y. Lu, Y. Mei, M. Ballauff, M. Drechsler, Thermosensitive core–shell particles as carrier systems for metallic nanoparticles, J. Phys. Chem. B 110 (2006) 3930–3937.
[8] M. Ballauff, Y. Lu, "Smart" nanoparticles: preparation, characterization and applications, Polymer 48 (2007) 1815–1823.
[9] Y. Lu, S. Proch, M. Schrinner, M. Drechsler, R. Kempe, M. Ballauff, Thermosensitive core–shell microgel as a "nanoreactor" for catalytic active metal nanoparticles, J. Mater. Chem. 19 (2009) 3955–3961.
[10] N. Welsch, M. Ballauff, Y. Lu, Microgels as nanoreactors: applications in catalysis, Adv. Polym. Sci. 234 (2010) 129–163.
[11] K. Esumi, R. Isono, T. Yoshimura, Preparation of PAMAM-and PPI-metal (silver, platinum, and palladium) nanocomposites and their catalytic activities for reduction of 4-nitrophenol, Langmuir 20 (2004) 237–243.
[12] H. Xu, J. Xu, Z. Zhu, H. Liu, S. Liu, In-situ formation of silver nanoparticles with tunable spatial distribution at the poly (N-isopropylacrylamide) corona of unimolecular micelles, Macromolecules 39 (2006) 8451–8455.
[13] N. Sahiner, In situ metal particle preparation in cross-linked poly (2-acrylamido-2-methyl-1-propansulfonic acid) hydrogel networks, Colloid Polym. Sci. 285 (2006) 283–292.
[14] N. Sahiner, H. Ozay, O. Ozay, N. Aktas, New catalytic route: hydrogels as templates and reactors for in situ Ni nanoparticle synthesis and usage in the reduction of 2-and 4-nitrophenols, Appl. Catal. A 385 (2010) 201–207.
[15] N. Sahiner, O. Ozay, N. Aktas, E. Inger, J. He, The on demand generation of hydrogen from Co–Ni bimetallic nano catalyst prepared by dual use of hydrogel: as template and as reactor, Int. J. Hydrogen Energy 36 (2011) 15250–15258.
[16] N.A. Peppas, J.Z. Hilt, A. Khademhosseini, R. Langer, Hydrogels in biology and medicine: from molecular principles to bionanotechnology, Adv. Mater. 18 (2006) 1345–1360.
[17] N. Sahiner, Soft and flexible hydrogel templates of different sizes and various functionalities for metal nanoparticle preparation and their use in catalysis, Prog. Polym. Sci. 38 (2013) 1329–1356.
[18] S. Wunder, F. Polzer, Y. Lu, Y. Mei, M. Ballauff, Kinetic analysis of catalytic reduction of 4-nitrophenol by metallic nanoparticles immobilized in spherical polyelectrolyte brushes, J. Phys. Chem. C 114 (2010) 8814–8820.
[19] J. Liu, J. Wang, Z. Zhu, L. Li, X. Guo, S.F. Lincoln, R.K. Prud'homme, Cooperative catalytic activity of cyclodextrin and Ag nanoparticles immobilized on spherical polyelectrolyte brushes, AIChE J 60 (2014) 1977–1982.
[20] S. Noël, B. Léger, A. Ponchel, K. Philippot, A. Denicourt-Nowicki, A. Roucoux, E. Monflier, Cyclodextrin-based systems for the stabilization of metallic(0) nanoparticles and their versatile applications in catalysis, Catal. Today 235 (2014) 20–32.
[21] B. Léger, S. Menuel, A. Ponchel, F. Hapiot, E. Monflier, Nanoparticle-based catalysis using supramolecular hydrogels, Adv. Synth. Catal. 354 (2012) 1269–1272.
[22] J. Zeng, Q. Zhang, J. Chen, Y. Xia, A comparison study of the catalytic properties of Au-based nanocages, nanoboxes, and nanoparticles, Nano Lett. 10 (2009) 30–35.